[CANCER RESEARCH 50, 700–709, February 1, 1990]

Characterization of Adenocarcinomas of the Dorsolateral Prostate Induced in Wistar Rats by *N*-Methyl-*N*-nitrosourea, 7,12-Dimethylbenz(*a*)anthracene, and 3,2′-Dimethyl-4-aminobiphenyl, following Sequential Treatment with Cyproterone Acetate and Testosterone Propionate[1]

Maarten C. Bosland,[2] Menk K. Prinsen, Theo J. M. Dirksen, and Ben J. Spit

Department of Biological Toxicology, TNO-CIVO Toxicology and Nutrition Institute, P. O. Box 360, 3700 AJ Zeist, The Netherlands

ABSTRACT

Carcinomas of the rat prostate induced by a single injection of *N*-methyl-*N*-nitrosourea, 7,12-dimethylbenz(*a*)anthracene, and 3,2′-dimethyl-4-aminobiphenyl, after sequential treatment with cyproterone acetate and testosterone propionate, were evaluated as potential animal models for prostatic cancer. All ten carcinomas examined were located in the dorsolateral prostate region and did not involve the distal parts of the seminal vesicles and coagulating glands. The incidence of urinary obstruction leading to the animals' death was 6 of 10 rats, and metastases in the lung, abdominal lymph nodes, and/or liver also occurred in 6 of 10 rats. The tumors were invasive adenocarcinomas, showing frequent perineural invasion and a variable degree of differentiation. There were ultrastructural similarities with human prostatic carcinomas, such as intracellular lumina. Plasma acid phosphatase was increased. Enzyme histochemical analysis revealed similarities with the Dunning R3327H and -HI prostatic carcinomas but was not helpful in determining the site of origin of the tumors. The gross and microscopic appearance of the tumors and the observation of preneoplastic lesions exclusively located in the dorsolateral prostate suggest this lobe as site of origin of the carcinomas. Preneoplastic lesions ($n = 9$) included atypical hyperplasias ($n = 5$) and lesions with all histological characteristics of carcinoma except for local invasion and metastases, which were classified as carcinoma *in situ* ($n = 4$). Although androgen sensitivity could not be assessed, the observed characteristics of the tumors [their long latency time (46–80 weeks), the presence of preneoplastic lesions, and the short duration of the treatment, leaving the animals intact] all indicate that the present approach is a valid animal model for the study of prostatic carcinogenesis.

INTRODUCTION

Animal model systems of carcinogenesis can greatly contribute to our understanding of human carcinogenesis. Using such models, carcinogenic agents can be identified, factors that modify the carcinogenic process can be studied under controlled conditions, and the mechanism of action of these agents and modifying factors can be addressed. It is of utmost importance that such models of carcinogenesis be well characterized and resemble their human counterparts in such key features as morphology and histogenesis, latency time and growth rate, and biological behavior.

Desired properties of animal models for the study of biology and therapy of prostatic cancer have been discussed by Coffey and Isaacs (1). The requirements of a model for the study of the genesis of prostatic cancer, however, have not been well defined in the literature. Based on the generalized properties of human prostatic cancer summarized by others (1–4) and on what is known about the etiology and pathogenesis of this neoplastic disease (5, 6), we have derived the following requirements for a rodent model for prostatic carcinogenesis: The adenocarcinomas should originate exclusively from the dorsolateral prostate,[3] because that part of the rodent prostate is most likely homologous to the region of the prostate from which prostatic cancer originates in man (8–11), as pointed out elsewhere (5, 12). The great majority of human carcinomas are androgen sensitive and respond to hormonal (estrogen) therapy followed by relapse to a hormone-insensitive state. This feature should also be a hallmark of an appropriate animal model. Biochemical characteristics of the carcinomas should be comparable to those of the human tumor, *e.g.*, the presence of androgen-metabolizing enzymes and androgen receptors. The slow growth rate and the pattern of metastatic spread to lymph nodes, lung, liver, and bone, characteristic of human prostatic cancer, should be features of such a model. Although a slow growth rate leading to long latency times is usually regarded as a disadvantage for practical animal models for carcinogenesis, a model system for rapid induction of prostate carcinomas would compare unfavorably with the human situation. Two typical characteristics of advanced human prostate cancer, *i.e.*, elevation of serum acid phosphatase and urinary obstruction, should also occur. There is a great diversity in several of these properties of human prostatic cancer, particularly in the degree of histological differentiation, the pattern of progression and, to a lesser degree, hormone sensitivity. An appropriate animal model should mimic this diversity. Because of the central importance of androgen sensitivity for many of the human prostatic carcinomas, it is essential for a prostatic cancer model that the tumors can be induced in intact animals, *i.e.*, animals that are not castrated or otherwise hormonally manipulated. Environmental factors affecting the progression from early noninvasive, so-called latent carcinoma to invasively growing adenocarcinomas are probably critical determinants of human prostatic cancer risk (5). It is, therefore, highly desirable that early stages of prostatic carcinogenesis be identifiable in an animal model and that induction is possible with a single or short-term exposure to a carcinogenic treatment, so that aspects of promotion and progression can be studied.

In a companion paper (12), we describe the chemical induction of carcinomas and preneoplastic lesions in the rat prostate, using an approach that may provide a useful animal model to study prostatic carcinogenesis. The purpose of this paper is to describe in detail morphological and biological characteristics of these carcinomas and preneoplastic lesions. Furthermore, to aid in determining the accessory sex gland site of origin of the induced carcinomas, their enzyme histochemical properties were compared to those of normal rat accessory sex glands and

Received 2/16/89; revised 6/9/89, 9/25/89; accepted 10/26/89.

The costs of publication of this article were defrayed in part by the payment of page charges. This article must therefore be hereby marked *advertisement* in accordance with 18 U.S.C. Section 1734 solely to indicate this fact.

[1] Supported in part by grants CIVO 80-3 and CIVO 84-3 from the Netherlands Cancer Foundation, Koningin Wilhelmina Fonds.

[2] Present address: Institute of Environmental Medicine, New York University Medical Center, 550 First Avenue, New York, NY 10016. To whom requests for reprints should be addressed. This work was submitted as part of a dissertation to the State University of Utrecht, The Netherlands, in partial fulfillment of the requirements for the Doctorate Degree.

[3] Nomenclature of the male accessory sex glands is according to the system of Jesik *et al.* (7).

of the transplantable Dunning R3327H and R3327HI prostate carcinomas which are of proven dorsolateral prostate origin (13, 14). These two carcinoma lines were also used as positive controls for determining elevation of plasma acid phosphatase by the induced prostate carcinomas.

MATERIALS AND METHODS

Source of Tissue and Histological Procedures. The dorsolateral prostate adenocarcinomas and preneoplastic lesions that are discussed here were obtained from animals killed when moribund in the induction experiments described in a companion paper (12), as is summarized in Table 2. In these experiments, the carcinogens MNU,[4] DMBA, and DMABP were administered by a single injection during stimulation of prostatic cell proliferation by sequential treatment with cyproterone acetate and testosterone propionate. These procedures are described in detail in the companion paper (12). Necropsy procedures, fixation, tissue trimming, and histological methods used have also been detailed in this companion paper (12). For ultrastructural analysis, 3–5 mm^3 pieces of tumor tissue were fixed in 3% glutaraldehyde solution in 0.1 M sodium cacodylate (pH 7.2) at 4°C for 17 h and stored in 0.1 M sodium cacodylate buffer at 4°C until further processing. Postfixation was carried out in a 4% osmium tetraoxide solution in 0.1 M sodium cacodylate for 17 h. After dehydration, the tissue pieces were embedded in glycid ether-Araldite. Semithin sections were stained with methylene blue. Ultrathin sections were contrasted with uranyl acetate and lead citrate and examined using a Philips EM 201 G at 50 kV.

Plasma Acid Phosphatase. From 9 animals with macroscopically visible prostate tumors, blood was collected in heparinized tubes by cannulating the abdominal aorta while the animals were under ether anesthesia. Plasma was obtained by centrifugation (2000 × *g*), using Sure Sep (Organon Technika, Charlotte, NC), and stored at −20°C until assayed. Plasma acid phosphatase activity was determined according to Seiler and Nagel (15), using α-naphthyl phosphate as substrate. The tartrate-inhibitable fraction was calculated by subtracting the enzyme activity obtained in the presence of 0.0135 M *L*(+)-tartrate from the total activity.

Enzyme Histochemistry. From a number of dorsolateral prostatic tumors a representative, small piece (approximately 0.5 cm^3) was sampled for enzyme histochemistry, frozen in isopentane over liquid nitrogen, and stored at −80°C. Pieces of the Dunning R3327H and R3327HI tumors and of normal accessory sex glands of untreated young adult male Cpb:WU rats were sampled in the same manner for comparative studies. Ten-μm-thick cryostat sections were prepared and histochemical reactions for the following enzymes were carried out, using appropriate positive control tissues and inhibitors (16): GGT according to Rutenberg *et al.* (17); isopropyl alcohol dehydrogenase using the procedure of Hardonk (18); acid phosphatase by the lead nitrate method of Gomori with β-glycerophosphate as substrate (16); glucose-6-phosphatase as described by Wachstein and Meisel (19); succinic dehydrogenase by the procedure of Nachlas *et al.* (20); alkaline phosphatase using Burstone's method with naphthol AS-BI as substrate (21); LAP according to the procedure of Nachlas *et al* (22); and 5′-nucleotidase by the method of Wachstein and Meisel (23). This panel of enzyme histochemical assays was selected to aid in determining the site of origin of the carcinomas, because these provide the greatest possible discrimination in histochemical (see Ref. 13) and biochemical (see Ref. 14) characteristics among the rat ventral, lateral, and dorsal prostate lobes. Staining intensity was scored blindly as absent, minimal, slight, moderate, or marked, and the distribution of the staining was recorded as focal or diffuse.

Dunning R3327H and R3327HI Prostatic Carcinomas. The Dunning R-3327H (androgen-sensitive) and R3327HI (androgen-insensitive) prostatic adenocarcinomas (see Ref. 14) were used as comparison for the chemically induced prostate carcinomas. These tumors were generously donated by Dr. N. H. Altman (Papanicolaou Cancer Research Institute, Miami, FL) together with breeding pairs of the Copenhagen (COP) and Fischer (F344) rat strains. The tumors were maintained in young adult male F344 × COP F_1 rats; the R3327H tumor in intact animals and the R3327HI tumor in castrates. The tumors were transplanted before they reached a volume of 4 cm^3, by implanting pieces of approximately 0.5 mm^3 s.c. on both flanks of each animal using a trocar method (16–18-gauge needle; 1 ml L-15 medium). Histological appearance and hormone sensitivity were routinely examined to monitor tumor stability and appeared comparable to what has been reported by others (13, 14). Material from the R3327HI tumor for enzyme histochemistry and plasma for acid phosphatase determination were taken from intact animals bearing tumor transplants.

Statistical Methods. The plasma acid phosphatase data were statistically evaluated using Student's *t* test and linear regression analysis. The correlations between tumor size and acid phosphatase activity and between tumor size and latency were determined by calculating the Spearman rank correlation coefficient. A one-tailed *P* value of 0.05 or smaller was considered significant.

RESULTS

Characteristics of ten carcinomas and nine preneoplastic epithelial lesions of the dorsolateral prostate are described in this report (Table 1). These lesions had been induced by the chemical carcinogens MNU, DMBA, and DMABP as described elsewhere (12). Nine of the ten carcinomas were grossly apparent (Table 1). The latency time (time after carcinogen administration) of these 10 carcinomas was 64 ± 4 (SEM) weeks (range, 46–80 weeks).

Gross Observations

Six of the nine grossly visible tumors (67%) were symmetrically located in the region of the dorsolateral prostate, involving not only the dorsolateral prostate lobes but also the base of both seminal vesicle/coagulating gland complexes. Two of these tumors had caused bilateral urinary obstruction and hydronephrosis, whereas the other four had caused unilateral obstruction of the urinary flow (Fig. 1). Three tumors (33%) were located on one side of the dorsolateral prostate involving the base of the seminal vesicles and coagulating glands on that side. These tumors did not cause urinary obstruction, and they were smaller (diameter, 1.67 ± 0.17 cm; range, 1.5–2.0 cm) than the symmetrically located tumors (diameter, 3.40 ± 0.51 cm; range, 2–5 cm). There was no statistically significant correlation between tumor size and tumor latency. Smaller tumors were single masses, whereas some larger tumors had a multinodular ap-

Table 1 *Types of dorsolateral prostate epithelial proliferative lesions and histological and clinical characteristics of adenocarcinomas of the dorsolateral prostate by inducing agent*[a]

	MNU	DMBA	DMABP	Total
Atypical hyperplasia	2	0	3	5
Carcinoma *in situ*	2	1	1	4
Adenocarcinoma, total	7	1	2	10
Size				
Microscopic	1	0	0	1 (10)[b]
Grossly apparent	6	1	2	9 (90)
Degree of differentiation				
Well differentiated	1	1	1	3 (30)
Moderately differentiated	3	0	1	4 (40)
Poorly differentiated	3	0	0	3 (30)
Incidence of metastases				
Total	5	0	1	6 (60)
Lung	4	0	0	4 (40)
Lung and abdominal cavity	0	0	1	1 (10)
Lung, liver, and abdominal cavity	1	0	0	1 (10)
Urinary obstruction	4	1	1	6 (60)

[a] See Ref. 12.
[b] Percentage of total is given in parentheses.

[4] The abbreviations used are: MNU, *N*-methyl-*N*-nitrosourea; DMABP, 3,2′-dimethyl-4-aminobiphenyl; DMBA, 7,12-dimethylbenz(*a*)anthracene; GGT, γ-glutamyl transpeptidase; LAP, leucine aminopeptidase.

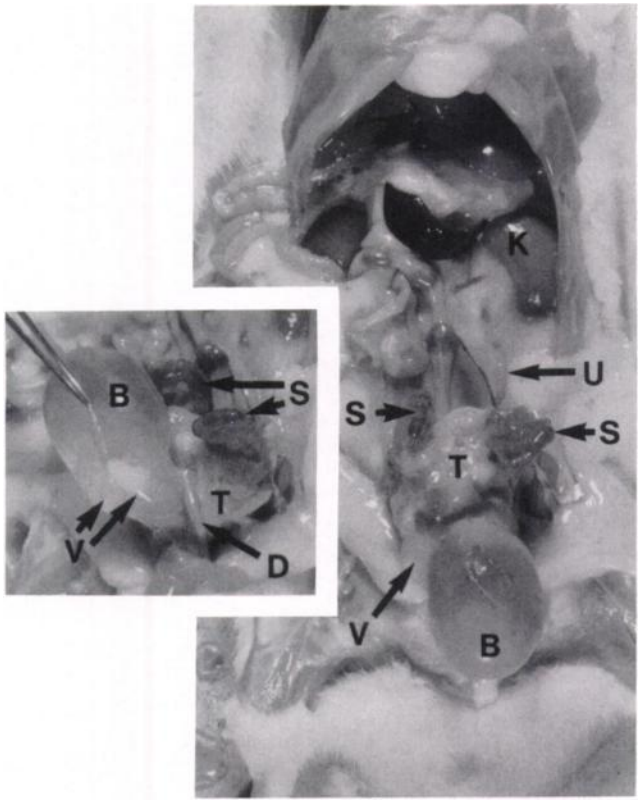

Fig. 1. Tumor located in the region of the dorsolateral prostate. This tumor (*T*), diagnosed as adenocarcinoma, grossly involved all of the dorsolateral prostate and the base of the seminal vesicle-coagulating gland complexes (*S*), which were swollen. The ventral prostate (*inset*; *V*) was not involved. The urinary bladder (*B*) and ureters (*U*) were distended, because of obstruction of the urinary flow, and the kidneys (*K*) were mildly hydronephrotic.

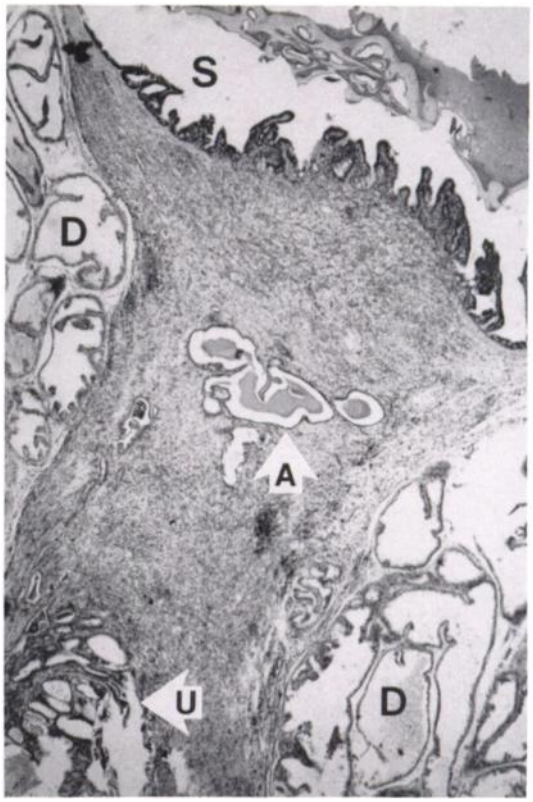

Fig. 2. Microscopic adenocarcinoma located in the dorsolateral prostate region. This poorly differentiated carcinoma involved the dorsal prostate (*D*), seminal vesicle (*S*), ampullary gland (*A*), and prostatic utricle (*U*). H & E, × 30.

pearance. The tumors all had a firm consistency and were white-gray and homogeneous of texture on the cut surface. Distinct central necrosis was present in two large tumors, and two others showed a translucent exudate on the cut surface. The seminal vesicles and coagulating glands that were involved in the tumor processes were swollen, suggesting obstruction of drainage of secretion (Fig. 1). The ventral prostate lobes were never grossly involved in the tumors (Fig. 1).

Histopathology

Carcinomas. All ten tumors were adenocarcinomas with a glandular growth pattern. The carcinomas histologically involved the dorsal and/or lateral prostate lobes and at least one other accessory sex gland, in all cases. Most tumors histologically involved all of the accessory sex gland structures that are associated with the dorsolateral lobes: ampullary glands, seminal vesicles and coagulating glands, including the excretory ducts of these glands. Even the one microscopic carcinoma involved several of these structures (Fig. 2). (Interestingly, a microscopic carcinoma exclusively located in the dorsolateral prostate was observed in an experiment using the same approach to induce prostatic cancer as was applied here (12), with MNU as inducing agent.[5]) All ten carcinomas grew invasively, and several showed perineural invasion (Fig. 3). The architecture of the dorsolateral prostate region was often markedly disturbed.

The degree of histological differentiation of the carcinomas varied considerably, both within a single carcinoma and between carcinomas (Table 1), ranging from well (Fig. 4) to moderately

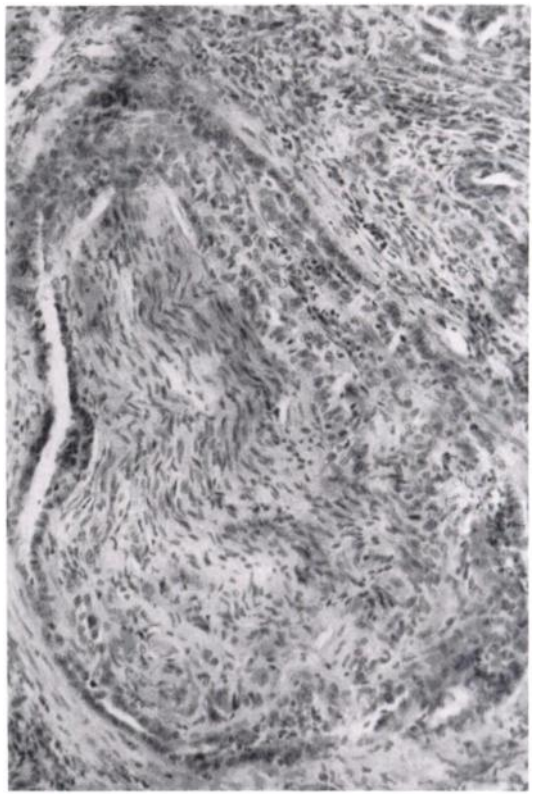

Fig. 3. Invasion of the perineural space of a nerve bundle in the dorsolateral prostate by a moderately differentiated prostatic adenocarcinoma. H & E, × 145.

(Fig. 5) to poorly (Fig. 6) differentiated. The carcinomas were graded into these three categories according to the growth pattern that predominated (4). Carcinomas with a generally

[5] M. C. Bosland, unpublished observation.

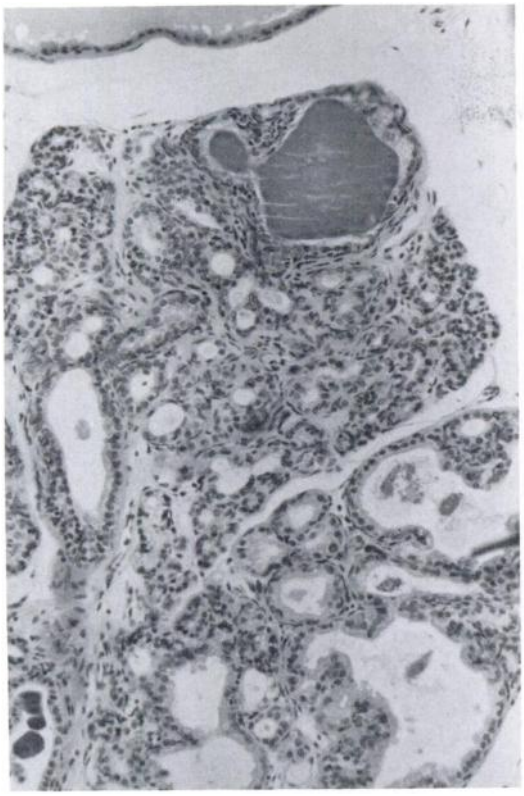

Fig. 4. Well differentiated adenocarcinoma exclusively located in the dorsal and lateral prostate. Note the normal prostatic epithelium at the top; the haphazardly arranged, small to very small neoplastic glands, some of which contain secretum; and the increased amount of fibromuscular stroma. H & E, × 120.

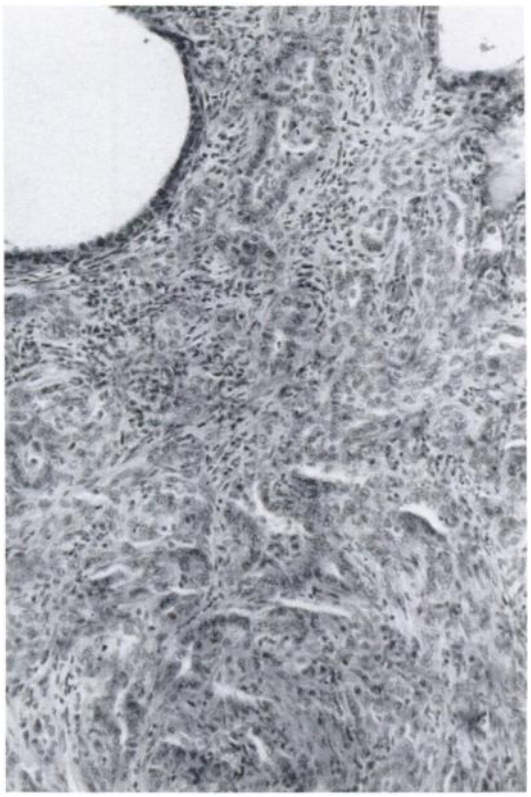

Fig. 5. Moderately differentiated carcinoma of the dorsolateral prostate. Note the normal dorsolateral prostate acini in the *upper right* and *left hand corners* and the abundant stroma containing inflammatory cells. H & E, × 120.

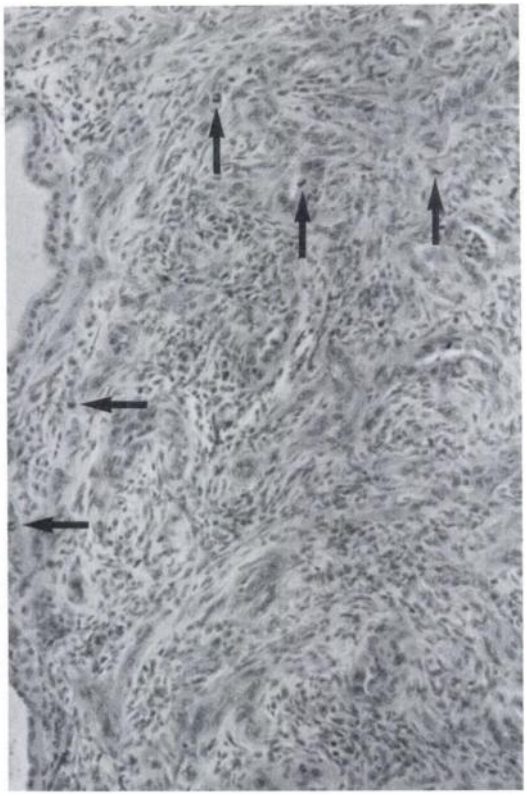

Fig. 6. Poorly differentiated adenocarcinoma of the dorsolateral prostate. There are only few recognizable glandular structures. Note the normal acinar epithelium at the *left* and the many mitotic figures (*arrows*). H & E, × 120.

well developed acinar growth pattern were considered well differentiated, whereas carcinomas with predominantly poorly developed acini were classified as moderately differentiated. Carcinomas with little evidence of acinar structures were considered poorly differentiated. With decreasing degree of differentiation there was an increase in cellular anaplasia: loss of cellular polarity; variation in cellular and nuclear size and shape and in cytoplasmic/nuclear ratio (pleomorphism); and changes in nuclear chormatin distribution and in staining properties and texture of cells and nuclei. There was no apparent correlation between degree of differentiation and size or latency time of the carcinomas.

General features of all carcinomas listed in Table 1 were the presence of abundant fibrous stroma and acini consisting of a single layer of neoplastic cells without basal cells (Figs. 4–6). A marked mixed inflammatory cell infiltrate in interstitium and acinar lumina was often but not always present (Figs. 5 and 6). In a very well differentiated microscopic carcinoma found in the earlier mentioned experiment,[5] the mildly atypical neoplastic epithelium had somewhat retained its cellular polarity and secretory properties. The main differences with normal dorsolateral prostate were a marked focal increase in the number of acini, a much smaller size of the neoplastic acini, which were disorderly arranged, sometimes back-to-back, and a slightly increased amount of fibromuscular stroma (Fig. 4). The three well differentiated carcinomas listed in Table 1 had acini that were small and varied from round or oval to tubular and that displayed a disturbed acinar-stromal relation. The epithelium had mostly lost its normal cellular polarity and showed little or no evidence of secretory activity. The cells and nuclei were somewhat pleomorphic. The five moderately differentiated carcinomas predominantly consisted of small acini, mostly tubular or slit-like, with no evidence of secretory activity (Fig. 5). The

cells had completely lost normal polarity and showed a moderate degree of pleomorphism. They were generally cuboidal and slightly hyperbasophilic with enlarged, hypochromatic nuclei, as was also observed for most well and all poorly differentiated carcinomas. In the two poorly differentiated carcinomas most moderately to markedly anaplastic cells were arranged in small clusters or strands amid abundant stroma, and mitotic activity was higher than in well or moderately differentiated carcinomas in which very few mitotic figures occurred (Fig. 6).

Electron microscopy revealed fewer differences between well, moderately, and poorly differentiated carcinomas than light microscopy. Even the one poorly differentiated carcinoma examined showed a tendency to form lumina, but the microvilli on the luminal side of the cells were less well developed in moderately to poorly differentiated carcinomas than in well differentiated tumors (Fig. 7). Desmosomes and junctional complex-like structures were always found (Fig. 7), and sometimes there were obvious tonofilaments (Fig. 8). Structures suggestive of secretory vacuoles (Figs. 7 and 9), which normally occur in prostate secretory epithelial cells (24), were present in all tumors, even in histologically moderately to poorly differentiated carcinomas. Sometimes hyperplastic Golgi complexes, lipid droplets, and lysosomes were seen (Fig. 8). Polarization of the secretory and Golgi structures toward the apical side of the cell found in normal prostate secretory epithelium (24) was disturbed. Mitochondria were often changed, showing loss of cristae and occasional membranous inclusions (Figs. 7 and 8). Fragments of a basement membrane were present in well differentiated carcinomas but were less conspicuous or absent in moderately and poorly differentiated tumors. Distinct features

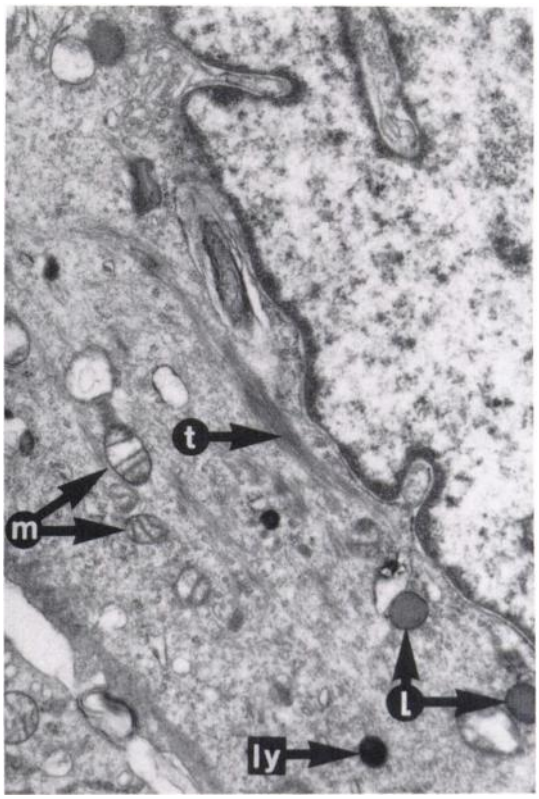

Fig. 8. Electron micrograph of a dorsolateral prostate adenocarcinoma cell showing tonofilaments (*t*), mitochondria with altered cristae (*m*), lipid droplets (*l*), lysosome-like structures (*ly*), and cytoplasmic inclusions in the nucleus. × 9500.

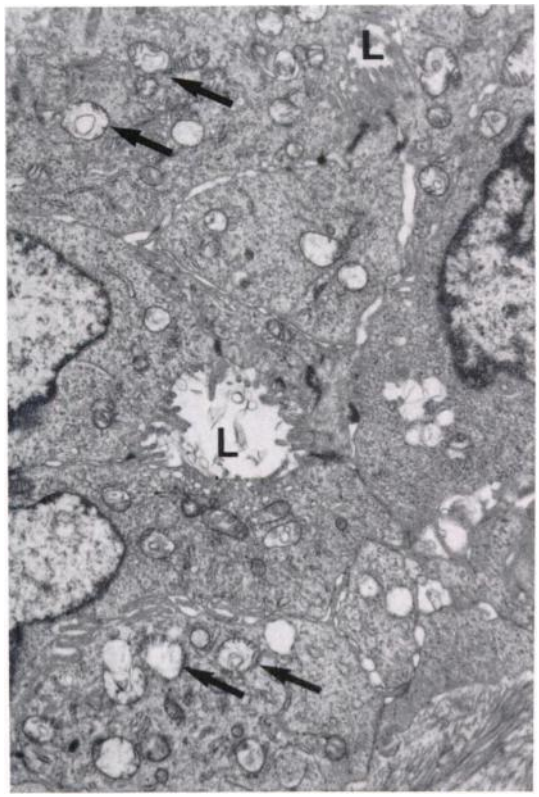

Fig. 7. Electron micrograph of a moderately-poorly differentiated adenocarcinoma of the dorsolateral prostate. There are poorly developed lumina (*L*) with microvilli and some secretory vacuole-like vesicles at the luminal side of the cells. Note the many mitochondria with disrupted cristae and membranous inclusions (*arrows*) and the junctional complex- and desmosome-like structures at the cell junctions. × 7200.

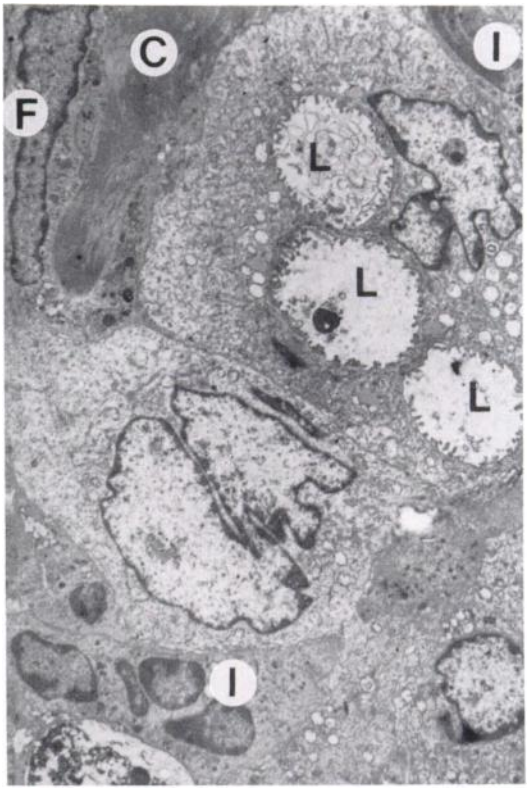

Fig. 9. Electron micrograph of a poorly differentiated dorsolateral prostate adenocarcinoma. One of the cells has intracellular lumina (*L*), one of which is filled with membranous structures. Note the highly irregular shape of the nuclei and the many secretory vacuole-like vesicles. There are stromal polymorphonuclear inflammatory cells (*I*), fibroblasts (*F*), and collagen (*C*). × 6000.

Fig. 10. Carcinoma *in situ* located in the periphery of the dorsal prostate (*D*), close to the lateral prostate (*L*). The lesion seems to involve an area of the size of 2–3 acini, and it is surrounded by an increased amount of fibromuscular stroma. It was found in only one of the step sections made at 250 μm distance. The growth pattern seems predominantly microglandular, and some glands contain secretory material. H & E, × 60.

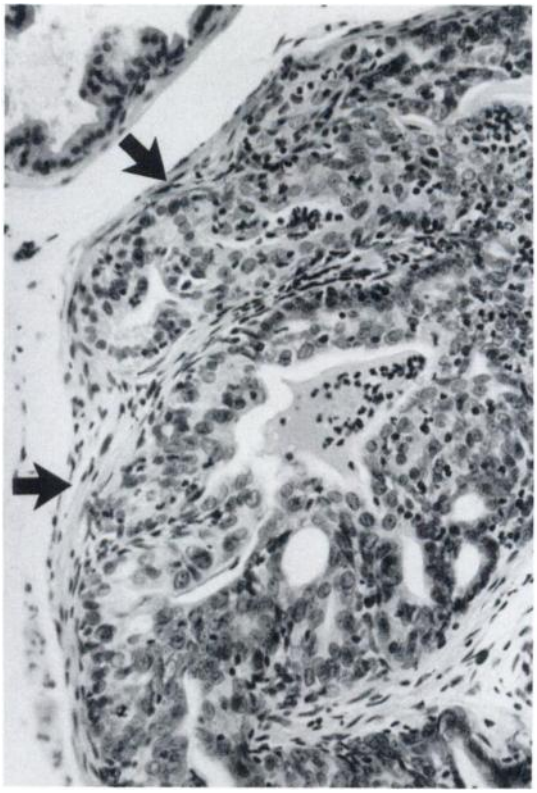

Fig. 11. Detail of Fig. 10. There is distinct cellular atypia in this lesion. It consists mainly of microglands, but there is also some cribriform growth and piling up of cells. Note the many interstitial and intraluminal inflammatory cells, intraluminal secretum, and the desmoplastic reaction (*arrows*). H & E, × 220.

were marked nuclear abnormalities: irregular shape; infoldings of the nuclear membrane and cytoplasmic inclusions; and clumping and condensation of chromatin along the nuclear envelope (Figs. 7–9), regardless of the degree of histological differentiation. The presence of intracellular lumina with distinct microvilli was another striking feature of some carcinomas (Fig. 9). The absence of basal cells seen by light microscopy was confirmed. The chemically induced carcinomas were ultrastructurally very similar to the Dunning R3327H and -HI carcinomas.

Carcinoma *in Situ*. Lesions that had all characteristics of carcinoma but lacked invasive growth were classified as carcinoma *in situ*. These lesions were small, occupying an area of the size of one to three acini. The acinar lumen was completely replaced by microglandular proliferation of mildly atypical cells (Figs. 10 and 11), which were indistinguishable from cells observed in well differentiated carcinomas. The glands were composed of a single layer of atypical cells without obvious basal cells. There was an often marked desmoplastic reaction surrounding the lesions, sometimes suggesting early invasive growth followed by reencapsulation (Fig. 11) and infiltrative growth from one acinus to an adjacent one (Fig. 10). There were occasional stromal septa within the lesions separating glandular structures, but back-to-back and cribriform-like arranged microglands were the predominant growth pattern (Fig. 11). Some inflammatory infiltrate was usually present (Fig. 11). The four such lesions seen in this study were all exclusively located in the dorsal and lateral prostate lobes and tended to be localized in the periphery of the gland (Fig. 10).

Atypical Hyperplasia. Lesions consisting of a hyperplasia of atypical cells that did not completely occupy one acinus were classified as atypical hyperplasia and thus coexisted with normal glandular epithelium. In all five cases observed in this study there was a mild increase in fibromuscular stroma surrounding the lesion. Two of these lesions had all cytological characteristics of carcinoma *in situ*, particularly the growth pattern of a single layer of cells forming microglands, and the apparent absence of basal cells. Two other lesions consisted of disorderly piled up, enlarged, hypochromatic cells that had partly lost their normal polarity and that had hypertrophic pale nuclei (Fig. 12). One lesion had characteristics of both types. The lesions were all located in the acini, not the ducts of the dorsal or lateral prostate lobes.

Metastases and Clinical Observations

Six of the ten carcinomas had metastasized to the lung (Fig. 13; Table 1). One had also disseminated the liver, and two had also metastasized to other structures in the abdominal cavity, such as mesenterial lymph nodes. Regional pelvic lymph node involvement was frequent; the available material did not allow determination of a precise incidence. No attempt other than a careful necropsy was made to detect bone metastases; none were grossly apparent. All six metastasizing carcinomas were moderately or poorly differentiated; well differentiated carcinomas did not metastasize. No correlation was apparent between metastasizing capacity and location or size of the tumors.

Urinary obstruction, due to blockage of the urinary flow by tumor growth through either the urethra or one or both ureters, was found in six cases (Fig. 1; Table 1). This caused unilateral or bilateral hydronephrosis and was the primary cause of morbidity in all six animals. Only larger, symmetrically located carcinomas caused urinary obstruction (see above).

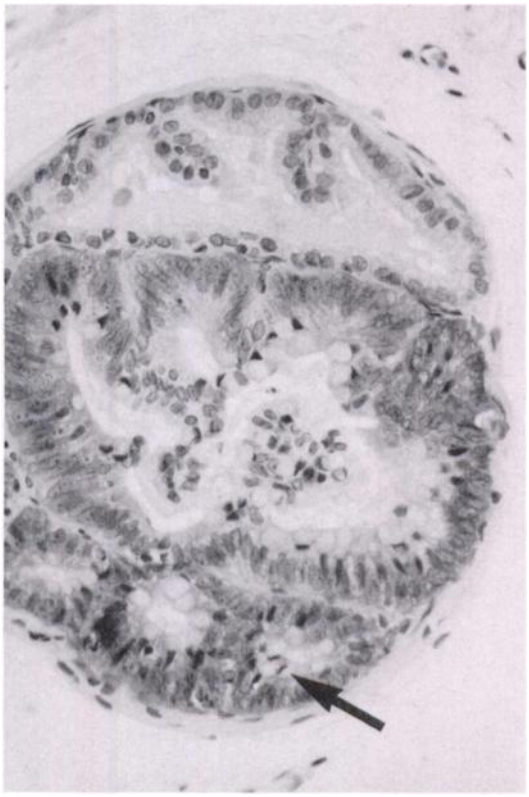

Fig. 12. Atypical hyperplasia in a dorsal prostate acinus consisting of piled-up cells displaying cellular atypia. The lesion is directly adjacent to normal acinar epithelium. Note the mitotic figure (*arrow*). H & E, × 300.

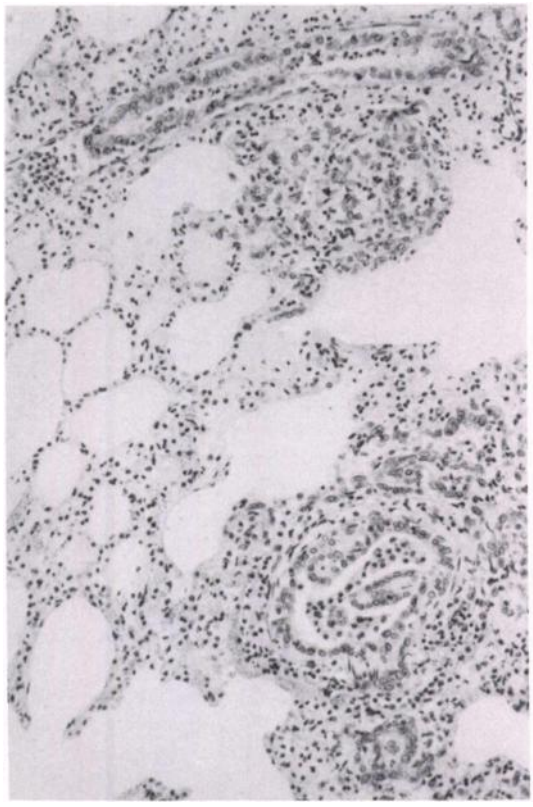

Fig. 13. Lung metastasis of dorsolateral prostate adenocarcinoma. There are intravascular and interstitial proliferating glandular structures in this somewhat autolytic lung. H & E, × 90.

Plasma Acid Phosphatase

Total and tartrate-inhibitible plasma acid phosphatase activity were significantly elevated in the group of animals with grossly apparent chemically induced prostatic carcinomas, as compared with controls (Table 2). There was no significant correlation between total or tartrate-inhibitible plasma acid phosphatase levels and size of the tumors (data not shown). For comparison, acid phosphatase activity was determined in plasma from animals bearing the Dunning R3327H and R3327HI carcinomas and from appropriate controls. Total acid phosphatase activity was significantly higher in R3327HI-bearing animals, but not in animals with the R3327H tumors, than in controls (Table 2); the tartrate-inhibitible fraction was borderline significantly elevated. The average tumor burden was somewhat higher in animals with R3327HI tumors than in R3327H tumor-bearing rats (Table 2). There was no significant correlation between total or tartrate-inhibitible plasma acid phosphatase activity and the tumor burden for either the R3327H or the R3327HI tumor-bearing animals.

Enzyme Histochemistry

Table 3 presents the results of the enzyme histochemical evaluation of normal rat male accessory sex glands, the R3327H and -HI tumors, and some of the chemically induced prostatic carcinomas. Useful markers for the various accessory sex glands appeared to be GGT, LAP and, to a lesser extent, isopropyl alcohol dehydrogenase, which is an indicator of 3β-hydroxysteroid dehydrogenase activity (18). GGT was a marker for the seminal vesicles and the ampullary glands and was negative in all other structures (Fig. 14, *a* and *b*). LAP was a marker for the lateral prostate (Fig. 14*c*) but was minimally active in the dorsal prostate and negative in all other glands examined (Fig. 14*d*). Isopropyl alcohol dehydrogenase was slightly positive in the lateral prostate and seminal vesicle. No GGT activity was found in the Dunning carcinomas. One-half of the chemically induced carcinomas examined were also negative for GGT. Two were diffusely minimally-moderately positive, whereas the two remaining carcinomas were partly negative and partly minimally-slightly positive. LAP and isopropyl alcohol dehydrogenase activity were found in the Dunning tumors and all chemically induced carcinomas examined, but the staining intensity varied.

Table 2 *Total and tartrate-inhibitable acid phosphatase activities in plasma from rats bearing chemically induced prostatic carcinomas or the Dunning R3327H and R3327HI transplantable prostatic carcinomas and from control animals*

Rats with prostatic carcinomas	*N*	Tumor burden (g)[a]	Acid phosphatase activity[b] Total	Tartrate inhibitable
Chemically induced	9	NA[c]	12.9 ± 4.5[d]	6.5 ± 1.1[d]
Cpb:WU controls[e]	15	NA	8.3 ± 0.7	3.9 ± 0.5
R3327H tumor	7	11.30 ± 1.93	23.5 ± 0.9	15.8 ± 1.2
R3327HI tumor	6	14.15 ± 3.11	31.5 ± 4.5[f]	24.8 ± 4.0[g]
F334 × COP controls	5	NA	18.4 ± 4.2	13.7 ± 4.1

[a] Only animals with R3327 tumors on both flanks were included in this study, and for each animal the total tumor burden (weight) was determined.
[b] Values are expressed in units/liter as mean ± SEM.
[c] NA, not applicable.
[d] $P < 0.02$ for difference with control value.
[e] Untreated animals of the same strain taken from an experiment carried out in the same period and which were killed at 75–80 weeks of age.
[f] $P < 0.05$ for difference with control value.
[g] $P = 0.067$ for difference with control value.

Table 3 *Enzyme histochemical properties of the rat male accessory sex glands, the Dunning R3327H and -HI prostate tumors, and chemically induced prostate carcinomas*

Enzyme	Dorsal prostate	Lateral prostate	Ventral prostate	Seminal vesicle	Coagulating gland	Ampullary gland	R3327H tumor	R3327HI tumor	Chemically induced carcinomas
γ-Glutamyl transpeptidase	−[a]	−	−	+++	−	++	−	−	− (4)[b] ±/++ (4)
Isopropyl alcohol dehydrogenase	−	±/−	++	±/−	NM	−	+	+	+ (6)
Acid phosphatase	++	++	++	++	++	++	+++	+	+/+++ (8)
Glucose-6-phosphate dehydrogenase	++	++	++	++	NM	NM	++	++	+/++ (6)
Alkaline phosphatase	++/+++	+	++	++/+++	NM	NM	++	++	±/++ (6)
Leucine aminopeptidase	−/±	++/+++	−	−	NM	NM	++/+++	+/++	+/+++ (6)
Succinic dehydrogenase	++	++	+	++	NM	NM	±/+	±/+	±/+ (6)
5′-Nucleotidase	±	++	++	±	NM	NM	++/+++	+/++	+/+++ (6)

[a] −, negative; ±, marginally positive; +, slightly positive; ++, moderately positive; +++, markedly positive; /, activity varied from the score before this sign to the score after this sign; NM, not measured.
[b] Numbers in parentheses, number of chemically induced carcinomas that were examined.

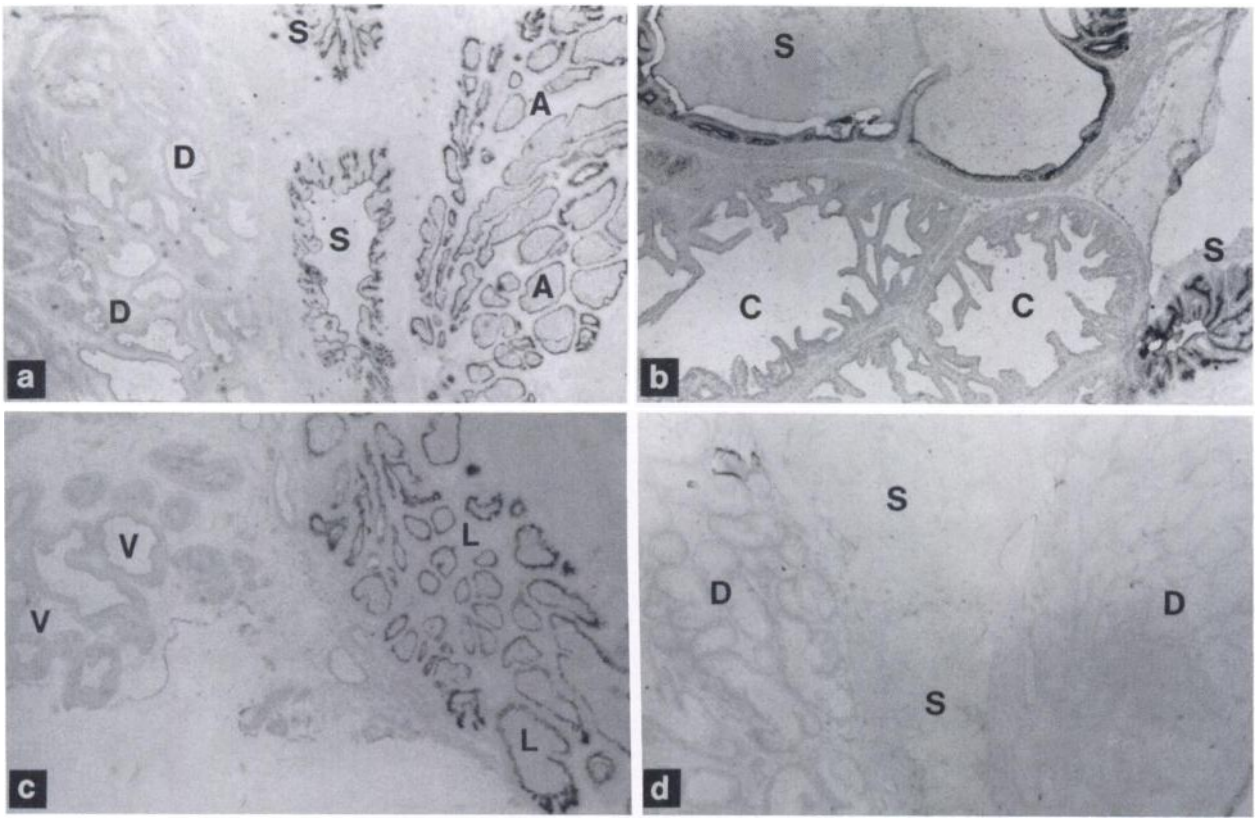

Fig. 14. Enzyme histochemical analysis. (*a*) GGT is positive in ampullary gland (*A*) and seminal vesicles (*S*) but negative in dorsal prostate (*D*). × 15. (*b*) GGT positive in seminal vesicle (*S*), but negative in coagulating gland (*C*). × 20. (*c*) LAP positive in lateral (*L*), but negative in ventral prostate (*V*). × 20. (*d*) LAP negative in dorsal prostate (*D*) and seminal vesicle (*S*). × 20.

DISCUSSION

The chemically induced carcinomas that were obtained in the experiments described in a companion paper (12) appeared to have a number of important characteristics that are desirable for an adequate animal model for the study of prostatic carcinogenesis. The tumors were adenocarcinomas. The generally long latent period and low mitotic activity indicate that these carcinomas were slow growing neoplasms. Plasma acid phosphatase activity was significantly elevated in animals with these carcinomas. The majority of these invasively growing tumors metastasized and caused urinary obstruction. There was a great diversity in characteristics such as tumor growth rate, as indicated by the latency time, and degree of histological differentiation. Probable precursor lesions were found, *i.e.*, carcinomas *in situ* and atypical hyperplasias, and induction was possible in intact animals with a single carcinogen administration. The material available for this study was not suitable to determine biochemical characteristics and hormone sensitivity of the carcinomas. These important aspects are addressed in ongoing studies. Other animal models of chemical (25, 26) and hormonal induction of prostatic cancer (27, 28) have not been characterized in detail.

The carcinomas all had a glandular growth pattern, as has the majority of the human prostatic carcinomas (4, 29, 30). Cribriform growth did not occur, unlike observations in some human carcinomas (4, 29, 30) and in carcinomas that occur spontaneously in the ventral prostate of aged rats (31), particularly in the ACI/segHapBR strain (32). The presence of abundant stroma and local invasion into the perineural spaces are two features of human prostatic cancer that were also observed in the chemically induced carcinomas (4, 30, 33). The light microscopic appearance of the carcinomas was comparable to that reported for spontaneously occurring (31, 34) and chemically (25, 26) or hormonally induced carcinomas of the rat

dorsolateral prostate(27, 28) and for transplantable carcinomas of rat dorsolateral prostate origin (13, 14, 27). Many ultrastructural features of human prostatic carcinomas (4, 29, 33) were also observed in the chemically induced tumors, *e.g.*, loss of basal cells, loss of cellular polarization, presence of lipid droplets, and formation of intracellular lumina. These intracellular lumina, which are a characteristic finding in moderately to poorly differentiated human prostatic carcinomas, have not been described before in reports on the ultrastructure of rat prostatic carcinomas (13, 35, 36). The ultrastructural evidence for the presence of secretory structures in the carcinoma cells suggests that the tumors originated from secretory alveolar cells and not from the epithelium of the excretory ducts, which does not have secretory properties, at least in the rat ventral prostate (37).

Nonneoplastic proliferative epithelial lesions, displaying cellular atypia and confined to one or a few alveoli, were exclusively found in the dorsolateral prostate; and they occurred only in treatment groups in which carcinomas of the dorsolateral prostate were observed as detailed elsewhere (12). Therefore, these lesions are considered likely precursors of dorsolateral prostatic carcinomas. Five of these lesions were classified as atypical hyperplasias and the others as carcinomas *in situ*. This classification is to some extent arbitrary, inasmuch as we examined only nine lesions and have no evidence for their premalignant nature. However, the degree of cellular atypica, the disorganization of normal glandular pattern and alveolar architecture, and the loss of normal epithelial-stromal relation that characterized these lesions all support the assumption that they are preneoplastic; similar criteria have been described to distinguish premalignant changes in the human prostate (30, 33, 38, 39). The lesions classified as carcinoma *in situ* lacked conspicuous basal cells. Because there is consensus in the literature about the requirement of absent basal cells for the diagnosis of malignancy in the human prostate (4, 29, 33, 38, 40, 41), this classification seems justified. Furthermore, these putative preneoplastic lesions in the rat dorsolateral prostate appeared to have morphological similarity to premalignant lesions described in the human prostate gland (4, 30, 39–42). It should be noted, however, that the carcinogenic treatments applied did not result in a high incidence of preneoplastic and low-grade malignant lesions relative to the incidence of clinical prostatic cancer (12), as occurs in humans, where the incidence of latent carcinoma is many times higher than that of the clinical disease (5, 8).

Most carcinomas had metastasized, primarily to regional lymph nodes and lung. This implies that both hematogenic and lymphogenic spread occurred, as is the case for human prostatic cancer (2–4). Metastases to bone, as is very frequent in humans, specifically to pelvic and spinal bones (3, 4), were not detected. Perhaps this is due to the insensitivity of our postmortem examination. However, among spontaneous (34), hormone-induced (27, 28), and chemically induced (25, 26) rat dorsolateral prostate carcinomas and transplantable tumor cell lines that were derived from such carcinomas (13, 14, 27, 44), metastatic ability is highly variable, with lymph node and lung metastases as the most frequent sites of dissemination; bony metastases have never been described. Therefore, there may be differences between human and rat models in the venous and/or arterial blood supply of pelvic and spinal bones or in other critical factors involved in the process of metastasis that lead to this apparent species difference.

The elevation of plasma acid phosphatase in rats with chemically induced carcinomas, most of which were advanced cancers comparable to stage C and D disease in humans, resembles the situation in humans. In comparison, animals bearing the Dunning R3327HI carcinomas also had elevated plasma acid phosphatase levels, but animals with the R3327H tumors did not. Isaacs *et al.* (14), however, reported elevated serum acid phosphatase levels both in animals with the R3327H tumor and the R3327HI tumor. Perhaps differences in total tumor burden or in assay methodology are responsible for these discrepancies. However, it is not likely that the small difference in tumor burden between rats with the rats with the R3327H and with the R3327HI tumor accounted for the difference in acid phosphatase elevation, because there was no correlation between total tumor weight per animal and plasma acid phosphatase activity.

The results of the histochemical analysis of normal prostate and the Dunning R3327H tumors are in agreement with those reported by others (13, 45), with some minor exceptions. There are no data in the literature on the enzyme histochemical properties of the R3327HI tumor, the seminal vesicles, and the coagulating and ampullary glands reported here. The enzyme activities in the R3327H and -HI tumors and in the chemically induced carcinomas were remarkably similar. However, the R3327 tumors were negative for GGT, whereas some of the chemically induced carcinomas were partly or completely positive. Because GGT appeared to be a marker for the seminal vesicle and ampullary gland, the possibility is raised that some carcinomas originated from one of these structures. The positive reaction of the carcinomas for LAP, on the other hand, contradicts such a notion; rather it points to the lateral prostate as a possible site of origin. Thus, the enzyme histochemical comparison between the chemically induced carcinomas and the various accessory sex glands does not appear to be helpful in determining the most likely site of origin of these tumors; a similar conclusion was reached by Smolev *et al.* (13) for the R3327H tumor.

In conclusion, the chemically induced rat prostatic carcinomas that are described here have a large number of important characteristics in common with human prostatic cancer, with the notable exception of the occurrence of bony metastases, while their androgen sensitivity remains to be investigated. Together with previously described features (12), these characteristics indicate that these chemically induced carcinomas are an appropriate model for human prostatic cancer and that the method for induction is thus a valid experimental approach for the study of human prostatic carcinogenesis.

ACKNOWLEDGMENTS

The authors wish to express their gratitude to Dr. H. E. Falke and J. Catsburg for carrying out the acid phosphatase assays; to G. Cook, F. van Welie, and B. Weir for their help with microphotography; to Dr. J. A. Joles for his editorial help, and to the histology staff of the Department of Biological Toxicology of the TNO-CIVO Toxicology and Nutrition Institute for their expert technical assistance. We thank Dr. N. H. Altman for providing animals carrying the Dunning tumors.

REFERENCES

1. Coffey, D. S., and Isaacs, J. T. Requirements for an idealized animal model of prostatic cancer. Prog. Clin. Biol. Res., *37:* 379–391, 1980.
2. Herr, H. W., and Yagoda, A. Neoplasms of the kidney, bladder and prostate. *In*: P. Calabresi, P. S. Schein, and S. A. Rosenberg (eds.), Medical Oncology, pp. 1045–1076. New York: The Macmillan Co., 1985.
3. Perez, C. A., Fair, W. R., Ihde, D. C., and Labrie, F. Cancer of the prostate. *In*: V. T. DeVita, S. Hellman, and S. A. Rosenberg (eds.), Cancer, Principles and Practice of Oncology, pp. 929–964. Philadelphia: J. B. Lippincott, Co., 1985.

4. Mostofi, F. K., and Price, E. B. Tumors of the Male Genital System. Washington, DC: Armed Forces Institute of Pathology, 1973.
5. Bosland, M. C. The etiopathogenesis of prostatic cancer with special reference to environmental factors. Adv. Cancer Res., *51:* 1–106, 1988.
6. Winkelstein, W., and Ernster, V. L. Epidemiology and etiology. *In*: G. P. Murphy (ed.), Prostatic Cancer, pp. 1–17. Littleton, MA: PSG Publishing Co., 1979.
7. Jesik, C. J., Holland, J. M., and Lee, C. An anatomic and histologic study of the rat prostate. Prostate, *3:* 81–97, 1982.
8. Breslow, N., Chan, C., Dhom, G., Drury, R. A. B., Franks, L. M., Gellei, B., Lee, Y. S., Lundberg, S., Spoarke, B., Sternby, N. H., and Tulinius, H. Latent carcinoma of prostate at autopsy in seven areas. Int. J. Cancer, *20:* 680–688, 1977.
9. McNeal, J. E. Origin and development of carcinoma of the prostate. Cancer (Phila.) *23:* 24–34, 1969.
10. Sandberg, A. A., Karr, J. P., and Muntzing, J. The prostates of dog, baboon and rat. *In*: E. Spring-Mills and E. S. E. Hafez (eds.), Male Accessory Sex Glands, pp. 565–608. Amsterdam: Elsevier/North Holland Biomedical Press, 1980.
11. Price, D. Comparative aspects of development and structure in the prostate. Natl. Cancer Inst. Monogr., *12:* 1–27, 1963.
12. Bosland, M. C., and Prinsen, M. K. Induction of dorsolateral prostate adenocarcinomas and other accessory sex gland lesions in male Wistar rats by N-methyl-*N*-nitrosourea, 7,12-dimethylbenz(*a*)anthracene, and 3,2′-dimethyl-4-aminobiphenyl after sequential treatment with cyproterone acetate and testosterone propionate. Cancer Res, *50:* 691–699, 1990.
13. Smolev, J. K., Heston, W. D. W., Scott, W. W., and Coffey, D. S. Characterization of the Dunning R3327H prostatic adenocarcinoma: an appropriate animal model for prostatic cancer. Cancer Treat. Rep., *61:* 273–287, 1977.
14. Isaacs, J. T., Heston, W. D. W., Weissman, R. M., and Coffey, D. S. Animal models of the hormone-sensitive and -insensitive prostatic carcinomas, Dunning R3327-H, R-3327-HI, and R-3327-AT. Cancer Res., *38:* 4353–4359, 1978.
15. Seiler, D., and Nagel, D. Saure Phosphatase in Serum (Substrat: α-Naphthylphosphat): Referenzwerte und diagnostische Aussage. J. Clin. Chem. Clin. Biochem., *21:* 519–525, 1983.
16. Pearse, A. G. E. Histochemistry, Vol. 1. Boston: Little, Brown & Co., 1968.
17. Rutenberg, A. M., Kim, H., Fischbein, J. W., Hanker, J. S., Wasserkrug, H. L., and Seligman, A. M. Histochemical and ultrastructural demonstration of γ-glutamyl transpeptidase activity. J. Histochem. Cytochem., *7:* 517–526, 1969.
18. Hardonk, M. J. A new method for the histochemical demonstration of steroid producing cells in human tissues. Histochemie, *5:* 234–243, 1965.
19. Wachstein, M., and Meisel, E. On the histochemical demonstration of glucose-6-phosphatase. J. Histochem., *5:* 592, 1956.
20. Nachlas, M. M., Tsou, K.-C., De Souza, E., Cheng, C.-S., and Seligman, A. M. Cytochemical demonstration of succinic dehydrogenase by the use of a new *p*-nitrophenyl substituted ditetrazole. J. Histochem., *5:* 420–436, 1957.
21. Burstone, M. S. Histochemical comparison of naphthol AS-phosphates for the demonstration of phosphatases. J. Natl. Cancer Inst., *20:* 601–615, 1958.
22. Nachlas, M. M., Crawford, D. T., and Seligman, A. M. The histochemical demonstration of leucine aminopeptidase. J. Histochem. Cytochem., *5:* 264–278, 1957.
23. Wachstein, M., and Meisel, E. Histochemistry of hepatic phosphatases at a physiologic pH. Am. J. Clin. Pathol., *27:* 13–23, 1957.
24. Lee, C., and Holland, J. M. Anatomy, histology, and ultrastructure (correlation with function), prostate, rat. *In:* T. C. Jones, U. Mohr, and R. D. Hunt (eds.), Genital System (Monographs on Pathology of Laboratory Animals), pp. 239–251. Berlin: Springer-Verlag, 1987.
25. Pollard, M. P., and Luckert, P. H. Production of autochthonous prostate cancer in Lobund-Wistar rats by treatments with *N*-methyl-*N*-nitrosourea and testosterone. J. Natl. Cancer Inst., *32:* 583–587, 1986.
26. Pour, P. M., and Stepan, K. Induction of prostatic carcinomas and lower urinary tract neoplasms by combined treatment of intact and castrated rats with testosterone propionate and *N*-nitrosobis(2-oxopropyl)amine. Cancer Res., *47:* 5699–5706, 1987.
27. Noble, R. L. Prostate Cancer of the Nb rat in relation to hormones. Int. Rev. Exp. Pathol., *23:* 113–159, 1982.
28. Pollard, M. P., Luckert, P. H., and Schmidt, M. A. Induction of prostate adenocarcinomas in Lobund Wistar rats by testosterone. Prostate, *3:* 563–568, 1982.
29. Kircheim, D., Brandes, D., and Bacon, R. L. Fine structure and cytochemistry of human prostatic carcinoma. *In*: D. Brandes (ed.), Male Accessory Sex Organs, pp. 397–423. New York: Academic Press, 1974.
30. Tannenbaum, M. Histopathology of the prostate gland. *In*: M. Tannenbaum (ed.), Urologic Pathology: The Prostate, pp. 303–397. Philadelphia: Lea & Febiger, 1977.
31. Bosland, M. C. Adenocarcinoma, prostate, rat. *In*: T. C. Jones, U. Mohr, and R. D. Hunt (eds.), Genital System (Monographs on Pathology of Laboratory Animals), pp. 252–260. Berlin: Springer-Verlag, 1987.
32. Ward, J. M., Reznik, G., Stinson, S. F., Lattirada, C. P., Longfellow, D. G., and Cameron, T. P. Histogenesis and morphology of naturally occurring prostatic carcinoma in the ACI/segHapBR rat. Lab. Invest., *43:* 517–522, 1980.
33. Altenahr, E., and Kastendieck, H. Proliferative patterns in prostatic carcinoma. *In*: E. Spring-Mills and E. S. E. Hafez (eds.), Male Accessory Sex Glands, pp. 437–455. Amsterdam: Elsevier/North-Holland Biomedical Press, 1980.
34. Pollard, M. Spontaneous prostate adenocarcinomas in aged germfree Wistar rats. J. Natl. Cancer Inst., *51:* 1235–1241, 1973.
35. Celesk, R. A., and Pollard, M.: Ultrastructural cytology of prostate carcinoma cells from Wistar rats. Invest. Urol., *14:* 95–99, 1976.
36. Seman, G., Myers, B., Bowen, M. M., and Dmochowski, L. Histology and ultrastructure of the R-3327 C-F transplantable prostate tumor of Copenhagen-Fischer rats. Invest. Urol., *16:* 231–236, 1978.
37. Ichihara, I., Kallio, M., and Pelliniemi, L. J. Light and electron microscopy of the ducts and their subepithelial tissue in the rat ventral prostate. Cell Tissue Res., *192:* 381–390, 1978.
38. Kastendieck, H., Altenahr, E., Husselmann, H., and Bressel, M. Carcinoma and dysplastic lesions of the prostate. A histomorphological analysis of 50 total prostatectomies by step-section technique. Z. Krebsforsch., *88:* 33–54, 1976.
39. Helpap, B. The biological significance of atypical hyperplasia of the prostate. Virchows Arch. A Pathol. Anat. Histol., *387:* 307–317, 1980.
40. Bostwick, D. G., and Brawer, M. K. Prostatic intra-epithelial neoplasia and early invasion in prostate cancer. Cancer (Phila.), *59:* 788–794, 1987.
41. Kastendieck, H. Correlations between atypical hyperplasia and carcinoma of the prostate. Pathol. Res. Pract., *169:* 366–387, 1980.
42. McNeal, J. E., and Bostwick, D. G. Intraductal dysplasia: a premalignant lesion of the prostate. Hum. Pathol., *17:* 64–71, 1986.
43. Drago, J. R., Goldman, L. B., Maurer, R. E., Eckels, D. D., and Gershwin, M. E. Histology, histochemistry, and acid phosphatase of Noble (Nb) rat prostate adenocarcinoma and treatment of an androgen-dependent Nb rat prostate adenocarcinoma. J. Natl. Cancer Inst., *64:* 931–937, 1980.
44. Lubaroff, D. M., Canfield, L., Feldbush, T. L., and Bonney, W. W. R3327 adenocarcinoma of the Copenhagen rat as a model for the study of the immunologic aspects of prostate cancer. J. Natl. Cancer Inst., *58:* 1677–1689, 1977.
45. Muntzing, J., Saroff, J., Sandberg, A. A., and Murphy, G. P. Enzyme activity and distribution in rat prostatic adenocarcinoma. Urology *11:* 278–282, 1978.